Check for updates

*Original Research Article*

# Impact of Resveratrol on Arrhythmias in Chronic Ischemic Heart Failure: Insights from Biochemical, Molecular, and Histopathological Studies in a Rat Model

Pharmacognosy Magazine
22(4) 1381–1390, 2026
© The Author(s) 2025
Article reuse guidelines:
in.sagepub.com/journals-permissions-india
DOI: 10.1177/09731296251400033
journals.sagepub.com/home/phm
Sage

**He Jing[1], Fuxian Wei[2] and Yan Wang[3]**

## Abstract

**Background:** Ventricular arrhythmias (VAs) frequently arise as complications in chronic ischemic heart failure (CIHF).
**Objectives:** We evaluated the effectiveness of resveratrol (RES) in a CIHF-induced rat model of VAs and explored the underlying mechanisms.
**Materials and Methods:** Animals received the left anterior descending coronary artery ligation to simulate CIHF and were subsequently treated daily with RES for 2 months. The subjects were categorized into five groups: normal control, VAs model, VAs model receiving simvastatin, and VAs models treated with RES at doses of 10 and 50 mg/kg. Key lipid factors, including high-density lipoprotein cholesterol (HDL-C), total cholesterol (TC), low-density lipoprotein cholesterol (LDL-C), and triglycerides (TG), were evaluated using a biochemical analyzer. Serum concentrations of inflammatory markers like interleukin-1β (IL-1β), interleukin-8 (IL-8), 6-keto-PGF1α, TXB2, endothelin (ET), and nitric oxide (NO) were quantified through radioimmunoassay (RIA). Real-time polymerase chain reaction (PCR) analyzed the VCAM-1, ICAM-1, and caspase-3 expression in the left anterior descending coronary artery, and Kv4.2, Cav1.2, and nerve growth factor (NGF) in the left ventricle.
**Results:** RES treatment led to significant improvements ($p < .05$) in lipid profiles, characterized by decreased concentrations of LDL-C, TG, and TC, alongside an elevation in HDL-C. Additionally, RES significantly ($p < .05$) lowered inflammatory cytokines and the ICAM-1 and VCAM-1 expression, while enhancing the Cav1.2, Kv4.2, and NGF expression ($p < .05$). Furthermore, RES significantly ($p < .05$) elevated 6-keto-PGF1α concentrations and increased ET and TXB2 levels.
**Conclusion:** RES emerges as an appropriate candidate for treating VAs.

## Keywords

Apoptosis, ventricular arrhythmias, chronic ischemic heart failure, rat, resveratrol

**Received** 03 June 2025; **revised** 16 September 2025; **accepted** 04 November 2025

## Introduction

In recent years, advancements in reperfusion treatment and improved treatments for acute arrhythmias after infarction have led to enhanced survival rates among patients experiencing acute myocardial infarction (MI) (Liu et al., 2024; Salari et al., 2023). Despite this progress, there is a notable increase in the incidence of ventricular arrhythmias (VAs) and subsequent sudden cardiac death (SCD) due to chronic ischemic heart failure (CIHF) linked to MI (Guo et al., 2021). Both clinical and animal research indicate an increase in the likelihood of developing CIHF by MI, which is primarily responsible for SCD (Theodorakis et al., 2025; Xiang et al., 2023). However, developing targeted therapies to reduce arrhythmia vulnerability in CIHF patients is still a significant issue. In contrast to the arrhythmias observed in the acute phase following MI, which primarily arise from disruptions in electrical uncoupling and resting membrane potential, the mechanisms underlying arrhythmias in CIHF are not well understood (Czyż et al., 2022). One potential therapeutic approach involves inhibiting neural remodeling. When heart failure presents with systolic dysfunction, there is an adaptive activation of the sympathetic nervous system aimed at

He Jing and Fuxian Wei contributed equally to this work.
[1]Department of Nuclear Medicine, Affiliated Hospital of Beihua University, Jilin City, Jilin, China
[2]Department of Pharmacy, Fenggang Hospital of Dongguan City, Dongguan, Guangdong, China
[3]Department of Cardiology, Xi'an Gaoling Hospital, Shaanxi, Xi'an, China

**Corresponding author:**
Yan Wang, Department of Cardiology, Xi'an Gaoling Hospital, Shaanxi, Xi'an 710200, China.
E-mail: wangyan071141@outlook.com

Creative Commons Non Commercial CC BY-NC: This article is distributed under the terms of the Creative Commons Attribution-NonCommercial 4.0 License (http://www.creativecommons.org/licenses/by-nc/4.0/) which permits non-Commercial use, reproduction and distribution of the work without further permission provided the original work is attributed as specified on the SAGE and Open Access pages (https://us.sagepub.com/en-us/nam/open-access-at-sage).

preserving normal cardiac output (Mavrogeni et al., 2022). However, if the reaction becomes excessive, the VA risk escalates. The left stellate ganglion stimulation possesses a pro-arrhythmic property (Liu et al., 2021). In animal studies, cardiac sympathetic denervation has been found to reduce the occurrence of VAs and ventricular tachyarrhythmias (VTs) associated with CIHF. Conversely, vagus nerve chronic electrical stimulation has been shown to increase the threshold for ventricular fibrillation in ambulatory dogs (Aguilar et al., 2025; Xiang et al., 2023).

CIHF is closely associated with alterations in lipid profiles, particularly triglyceride (TG), high-density lipoprotein cholesterol (HDL-C), total cholesterol (TC), and low-density lipoprotein cholesterol (LDL-C). Increased LDL-C concentrations are associated with the progression of atherosclerosis, causing coronary artery disease and subsequent cardiac failure, while HDL-C is recognized for its protective effects against cardiovascular diseases through reverse cholesterol transport (Wittenbecher et al., 2021). Dyslipidemia, characterized by high TC and TG levels, exacerbates inflammation and oxidative stress, promoting the development of VAs. The inflammatory milieu in CIHF is marked by elevated concentrations of cytokines, like interleukin-8 (IL-8) and IL-1β, which promote myocardial inflammation, fibrosis, and apoptosis. Pathways involving 6-keto-PGF1α, thromboxane B2 (TXB2), endothelin (ET), and nitric oxide (NO) play crucial roles in vascular function and cardiac remodeling, with increased TXB2 indicating heightened thromboxane synthesis that can lead to vasoconstriction and platelet aggregation, complicating heart failure (Zhao et al., 2021). Conversely, NO acts as a vasodilator, though its bioavailability may be compromised in heart failure, impairing endothelial function. In CIHF, the expression of adhesion molecules, vascular cell adhesion molecule-1 (VCAM-1) and intercellular adhesion molecule-1 (ICAM-1), is upregulated, facilitating leukocyte infiltration into the myocardium and exacerbating inflammation and myocardial damage (Singh et al., 2023). Additionally, caspase-3, a key mediator of apoptosis, is activated in response to cellular stress and inflammation, highlighting the interplay between these adhesion molecules and apoptotic pathways as critical in reducing the incidence of VAs (Lan et al., 2021). Furthermore, ion channels like Kv4.2 and Cav1.2 in the left ventricle are significant for cardiac action potential generation and conduction; alterations in their expression or function can lead to electrical instability and increased arrhythmia susceptibility (Wu et al., 2023). Nerve growth factor (NGF) has also been implicated in cardiac remodeling and arrhythmogenesis, enhancing sympathetic nervous system activity and contributing to the pro-arrhythmic state observed in heart failure. Understanding such molecular mechanisms can be used to develop targeted therapies aimed at restoring normal cardiac function and preventing arrhythmias in patients with CIHF (Dokshokova et al., 2022).

Resveratrol (RES) is a polyphenolic compound with significant pharmacological properties, demonstrating potential in modern medicine for its cardioprotective and neuroprotective effects. It has been shown to mitigate atherosclerosis by lowering LDL cholesterol, enhancing endothelial function, and exerting anti-inflammatory effects that protect against vascular damage (Raj et al., 2021). In cardiac tissues, RES can resist calcium overloading, inhibit myocyte apoptosis, alleviate the MI area, and reduce susceptibility against atrial fibrillation, making it a promising agent in ischemia/reperfusion (I/R) scenarios (Hosoda et al., 2023). Conversely, RES has been recognized for its ability to improve neuronal degeneration in Alzheimer's disease and reduce infarct size in cerebral I/R, highlighting its therapeutic potential in neuroprotection. Together, these compounds represent a multifaceted approach to addressing cardiovascular and neurodegenerative diseases, warranting further investigation into their mechanisms and clinical applications (Fan et al., 2022).

We investigated the impact of RES on VAs in CIHF rats and delved into the underlying mechanisms involved. This was accomplished through a comprehensive approach that integrated biochemical and molecular analyses to clarify how RES both prevents and treats VAs in this animal model.

## Materials and Methods

### *VAs Induction and Animal Grouping*

Fifty male Wistar rats (3 months old, 185 ± 15 g) were obtained from Xi'an Gaoling Hospital and kept in propylene cages under controlled environmental conditions. The temperature was set at 22°C ± 2°C, with a relative humidity of 36% ± 3%, and a dark/light cycle of 12 h each. The left anterior descending coronary artery was ligated to induce CIHF, and the rats were daily treated with RES for 2 months. Animals were randomly allocated to five groups of 10 animals: a normal control group (given 100 μL of isovolumic saline orally), a VAs model group, a VAs model group treated with simvastatin (20 mg/kg orally), and a VA model groups treated with RES at 10 and 50 mg/kg orally (Crowell et al., 2004; Kapetanovic et al., 2011; Liu et al., 2005). The research was approved by the Animal Experimental Administration of Xi'an Gaoling Hospital and was conducted based on the Guide for the Use and Care of Laboratory Animals. The VAs model was established using a well-documented rat model following MI. Following anesthetization using nalbuphine HCl (2 mg/kg) and pentobarbital sodium (3%, 0.3 mL/kg), animals underwent ventilation with room air using a respirator (KW-100-2, Karwin Biotechnology Company, China). The VAs groups underwent thoracotomy followed by left anterior descending coronary artery ligation, causing transmural MI. For 1 week, all rats received intramuscular penicillin injections (200,000 IU) two times a day. After the MI induction, follow-up was

performed following 2 months of standard feeding. Animals were excluded from the analysis if they exhibited any of the following conditions: (a) mortality occurring post-ligation, which indicated a failure in the surgical procedure or an inability to survive the induced MI; (b) failure to develop arrhythmias, as confirmed by continuous monitoring during the follow-up period; and (c) any significant complications arising from the surgical procedure that could affect the outcomes. After the study, following a 12-h fast, the rats were anesthetized using xylazine (100 mg/kg) and ketamine (15 mg/kg), and blood specimens were obtained via cardiac puncture for plasma and serum analysis (Lankin et al., 2022).

### *Analysis of Serum Lipid Profile*

An automatic biochemistry analyzer (GFD-800; Gaomi Caihong Analyzer Co., China) assessed serum TG, LDL-C, HDL-C, and TC levels, following the guidelines provided by the manufacturer (Qian et al., 2024).

### *Serum Inflammatory Cytokines*

Serum IL-8 and IL-1β levels were measured via radioimmunoassay (RIA) utilizing commercially available kits as instructed. Likewise, the concentrations of C-reactive protein (CRP) and TNF-α were evaluated through enzyme-linked immunosorbent assay (ELISA) using commercially supplied kits, following the established guidelines (Song et al., 2022).

### *Lipid Peroxidation (LPO) and Antioxidative Enzyme Activities*

LPO in both liver and serum tissues was analyzed using quantifying thiobarbituric acid-reactive substances (TBARS), with malondialdehyde (MDA) serving as the standard, based on the protocol by Naseri et al. (2019). Additionally, the catalase (CAT), glutathione peroxidase (GSH-Px), and superoxide dismutase (SOD) activity in liver and serum samples were assessed using, respectively, the chemical colorimetric, xanthine oxidase, and ammonium molybdate methods (Muñoz-Prieto et al., 2025).

### *NO, 6-keto-PGF1α, ET, and TXB2 Serum Levels*

The serum NO level was quantified by a commercially available kit as instructed. Similarly, plasma 6-keto-prostaglandin F1α (6-keto-PGF1α), ET, and TXB2 levels were assessed by RIA using commercially supplied kits (Chen et al., 2022).

### *Real-time Polymerase Chain Reaction (PCR)*

Total RNA isolation was done from 60 mg of tissue from the left anterior descending coronary artery and the left ventricle by adding TRIzol reagent (1 mL; Catalog No. 12183555; Invitrogen Inc., Germany), followed by a 2-min incubation at room temperature (25°C). For cDNA synthesis, 1,000 ng of total RNA from each tissue sample was combined with Takara Bio Mastermix (10 μL), random and oligo primers (1 μL), and deionized water (8 μL). The mixture was then subjected to reverse transcription using a thermal cycler (Thermo Fisher Scientific Inc., Germany) as follows: 10 min at 25°C, 45 min at 60°C, and 5 min at 60°C. For real-time PCR, 1,000 ng of cDNA was amplified with 1 μL each of reverse and forward primers targeting ICAM-1, VCAM-1, caspase-3, Cav1.2, Kv4.2, and NGF, combined with 8 μL of Takara Bio Mastermix. Reactions were performed on an Applied Biosystems QuantStudio 1 thermocycler (Chicago, USA) with 42 cycles at 60°C for 1 min each, and then melting curve analysis from 60°C to 95°C at 1°C/s. The ICAM-1, VCAM-1, and caspase-3 expression levels were quantified by the $2^{-\Delta\Delta Ct}$ method: ΔΔCt = [(Ct sample – Ct β-actin) – (Ct control – Ct β-actin)], and the fold change was calculated as $2^{-\Delta\Delta Ct}$. Primer3 software designed the primers (http://primer3.wi.mit.edu), and they were validated via NCBI Primer-BLAST (https://www.ncbi.nlm.nih.gov/tools/primer-blast/). Table 1 lists the primer sequences (Li et al., 2021). β-actin was the internal reference gene.

### *Kv4.2, Cav1.2, and NGF Protein Expression with Western Blotting*

Western blot analysis evaluated the Kv4.2, Cav1.2, and NGF expression levels. Tissue samples from the left ventricle were homogenized, with 100 mg of tissue combined with RIPA buffer (100 μL) and PBS (50 μL). After centrifugation, loading buffer (20 μL) was applied to a PVDF membrane, which then underwent incubation with primary antibodies against glyceraldehyde 3-phosphate dehydrogenase (GAPDH) (1:10,000; Abcam), Kv4.2 (1:1,000; Abcam), Cav1.2 (1:1,000; Abcam), and NGF (1:200; Abcam). Proteins were separated on a 10% SDS-PAGE gel. After being incubated for over 12 h at 4°C, the membrane was treated using an HRP-conjugated secondary antibody (1:1,000; Abcam) at 37°C for 40 min. An ECL reagent with the Image-Quant ECL Imager (GE Healthcare) visualized protein bands, then they were analyzed with Bio-Rad software and further processed using ImageJ (Bei et al., 2023).

### *Statistical Analysis*

Data analyses were performed by Statistical Package for the Social Sciences (SPSS) 16, employing one-way ANOVA followed by Duncan's *post hoc* test, with a significance level set at $p < .05$. The data normality was assessed with the Kolmogorov–Smirnov test, where a $p$ value >.05 suggested the normal data. Values are mean ± standard deviation (SD).

**Table 1.** Primer Sequences.

| Gene | Sequences (5′–3′) |
|---|---|
| β-actin | Forward: AGGCATCCTCACCCTGAAGTA<br>Reverse: CACACGCAGCTCATTGTAGA |
| Cav1.2 | Forward: GCTGGAGCTGATGCTGATG<br>Reverse: CTGGTGTTTCCGTCTCCTG |
| ICAM-1 | Forward: TGGAGAGCAAGAGGACACG<br>Reverse: TCCATGAGGAGGAACATCG |
| Kv4.2 | Forward: ATGGCTGAGCTGGAAGC<br>Reverse: CTGAGGTGAGGTGAGGTG |
| VCAM-1 | Forward: GCCAGGAGTATGAGGAAAGG<br>Reverse: TTGGGGTGTTGGTGGTGAG |
| NGF | Forward: GCTGCTGCTGCTGCTGTT<br>Reverse: GGTGGTGGTGGTGGTGTT |
| Caspase-3 | Forward: GAGCAAGGAGGAAGTGGA<br>Reverse: CAGTCCAGCAGGAGGAAAG |

## Results

### *Serum Levels of Serum Lipids*

The results indicated that the VAs group demonstrated significantly high TG, TC, and LDL-C levels versus the controls ($p < .05$). Simvastatin resulted in a significant reduction in TC, LDL-C, and TG versus the VAs group ($p < .05$). Furthermore, both 10 and 50 mg/kg doses of RES demonstrated a significant decrease in LDL-C and TC levels in comparison to the VAs group. However, TG concentrations remained unchanged with the 10 mg/kg RES treatment and were significantly reduced with the 50 mg/kg RES treatment. The HDL-C levels were comparable between the controls and the VAs + simvastatin group, but significantly lower in the VAs group ($p < .05$). Overall, RES demonstrated a beneficial effect on serum lipid profiles, particularly in reducing TC and LDL-C levels in rats subjected to VAs (Table 2).

### *Serum Inflammatory Cytokine Levels*

The analysis of serum inflammatory cytokines revealed significant differences among the study groups. The VAs group displayed elevated CRP, IL-8, TNF-α, and IL-1β concentrations in comparison to the normal group ($p < .05$). Simvastatin caused no significant reduction in these markers ($p > .05$). In contrast, 10 mg/kg RES caused a significant decrease in IL-8 and CRP concentrations in comparison to the VAs group ($p < .05$). Furthermore, the 50 mg/kg RES group exhibited even more pronounced reductions in CRP, IL-8, TNF-α, and IL-1β, all significantly lower in comparison to the VAs group ($p < .05$) (Table 3).

### *Antioxidative Enzyme Activities and Serum LPO Levels*

There was a significant difference across the groups. The VAs group exhibited markedly reduced levels of GSH-Px, T-SOD, and CAT, alongside elevated MDA levels versus the normal group ($p < .05$). Simvastatin did not significantly alter these parameters. However, administration of 10 mg/kg RES caused significant improvements in GSH-Px, T-SOD, and CAT concentrations, while also decreasing MDA in comparison to the VAs group ($p < .05$). Notably, the 50 mg/kg RES group demonstrated even greater enhancements in GSH-Px, T-SOD, and CAT activities, alongside a further reduction in MDA levels, all notably different from the VAs group ($p < .05$) (Table 4).

### *Serum 6-keto-PGF1α, ET, NO, and TXB2 Concentrations*

The analysis of serum NO, ET, TXB2, and 6-keto-PGF1α concentrations revealed significant differences among the study groups. The VAs group indicated significantly elevated concentrations of TXB2, NO, and ET, while 6-keto-PGF1α levels were notably reduced in comparison to the controls ($p < .05$). Simvastatin caused a significant reduction in TXB2 and ET levels, but NO levels remained elevated, and 6-keto-PGF1α levels were still significantly lower than normal. In contrast, administration of 10 mg/kg RES led to significant reductions in TXB2, NO, and ET levels, along with an increase in 6-keto-PGF1α versus the VAs group ($p < .05$). The 50 mg/kg RES group exhibited the most pronounced effects, with further decreases in TXB2, NO, and ET levels, and a significant increase in 6-keto-PGF1α, all versus the VAs group ($p < .05$) (Table 5).

### *VCAM-1, ICAM-1, and Caspase-3 Gene Expression*

The assessment of gene expression levels for ICAM-1, VCAM-1, and caspase-3 in the left anterior descending coronary artery revealed significant variations among the study

**Table 2.** Effect of RES on Serum Lipids (mmol/L).

| Group | TC | TG | HDL-C | LDL-C |
|---|---|---|---|---|
| Normal | 1.21 ± 0.4 | 0.23 ± 0.09 | 0.81 ± 0.09 | 0.14 ± 0.01 |
| VAs | 3.43 ± 0.6# | 1.06 ± 0.11# | 0.43 ± 0.03# | 0.39 ± 0.06# |
| VAs + simvastatin | 1.67 ± 0.2* | 0.52 ± 0.03* | 0.83 ± 0.06* | 0.29 ± 0.05* |
| VAs + 10 RES | 1.94 ± 0.2* | 0.64 ± 0.06 | 0.71 ± 0.04 | 0.24 ± 0.02* |
| VAs + 50 RES | 1.81 ± 0.4* | 0.52 ± 0.03* | 0.61 ± 0.05* | 0.18 ± 0.01* |

**Notes:** Values are mean ± SD, obtained from 10 rats. #$p < .05$, versus the normal group. *$p < .05$, versus the VAs group. HDL-C: High-density lipoprotein cholesterol; LDL-C: Low-density lipoprotein cholesterol; RES: Resveratrol; SD: Standard deviation; TC: Total cholesterol; TG: Triglycerides; VAs: Ventricular arrhythmias.

**Table 3.** Effect of RES on Serum Inflammatory Cytokines.

| Group | CRP (ng/L) | TNF-α (ng/L) | IL-8 (ng/mL) | IL-1β (ng/mL) |
|---|---|---|---|---|
| Normal | 3.21 ± 0.6 | 18.4 ± 1.3 | 1.61 ± 0.2 | 0.31 ± 0.06 |
| VAs | 7.11 ± 0.8# | 35.2 ± 2.4# | 3.03 ± 0.3# | 1.41 ± 0.16# |
| VAs + simvastatin | 8.51 ± 0.6 | 29.6 ± 3.1 | 3.64 ± 0.6 | 1.19 ± 0.11 |
| VAs + 10 RES | 6.11 ± 0.8* | 24.4 ± 2.7 | 3.01 ± 0.4* | 0.71 ± 0.19* |
| VAs + 50 RES | 5.21 ± 0.6* | 21.7 ± 2.2* | 2.11 ± 0.5* | 0.64 ± 0.09* |

**Notes:** Values are mean ± SD, obtained from 10 rats. #$p < .05$, versus the normal group. *$p < .05$, versus the VAs group. CRP: C-reactive protein; IL-8: Interleukin-8; IL-1β: Interleukin-1 beta; RES: Resveratrol; SD: Standard deviation; TNF-α: Tumor necrosis factor alpha; VAs: Ventricular arrhythmias.

**Table 4.** Effect of RES on Serum Lipid Peroxidation and Antioxidative Enzyme Activity.

| Group | T-SOD (U/mL) | GSH-Px (U/mL) | CAT (U/mL) | MDA (nmol/mL) |
|---|---|---|---|---|
| Normal | 133.4 ± 11.2 | 202.2 ± 14.2 | 5.92 ± 0.41 | 5.22 ± 0.27 |
| VAs | 66.4 ± 9.4# | 139.6 ± 11.2# | 2.15 ± 0.32# | 6.24 ± 0.27# |
| VAs + simvastatin | 72.2 ± 10.1 | 141.3 ± 10.5 | 2.21 ± 0.41 | 6.11 ± 0.32 |
| VAs + 10 RES | 86.2 ± 10.9 | 154.1 ± 9.2 | 3.02 ± 0.40 | 5.81 ± 0.32 |
| VAs + 50 RES | 120.1 ± 12.1* | 191.7 ± 9.28* | 3.43 ± 0.51* | 4.81 ± 0.42* |

**Notes:** Values are mean ± SD, obtained from 10 rats. #$p < .05$, versus the normal group. *$p < .05$, versus the VAs group. CAT: Catalase; GSH-Px: Glutathione peroxidase; MDA: Malondialdehyde; RES: Resveratrol; SD: Standard deviation; T-SOD: Total superoxide dismutase; VAs: Ventricular arrhythmias.

**Table 5.** Effect of RES on Serum Concentrations of NO, ET, 6-keto-PGF1α, and TXB2.

| Group | TXB2 (pg/mL) | NO (μmol/L) | ET (pg/mL) | 6-keto-PGF1α (pg/mL) |
|---|---|---|---|---|
| Normal | 50.24 ± 8.1 | 4.71 ± 0.94 | 171.2 ± 9.1 | 211.4 ± 14.7 |
| VAs | 202.4 ± 21.4# | 7.91 ± 0.84# | 311.6 ± 19.1# | 141.2 ± 12.1# |
| VAs + simvastatin | 181.2 ± 14.4* | 6.21 ± 1.06 | 232.4 ± 14.2* | 72.4 ± 11.4 |
| VAs + 10 RES | 141.5 ± 12.9* | 5.52 ± 0.85* | 221.4 ± 9.4* | 166.2 ± 14.2 |
| VAs + 50 RES | 91.2 ± 13.2* | 3.23 ± 0.74* | 151.2 ± 9.1* | 121.2 ± 11.2* |

**Notes:** Values are mean ± SD, obtained from 10 rats. #$p < .05$, versus the normal group. *$p < .05$, versus the VAs group. ET: Endothelin; NO: Nitric oxide; RES: Resveratrol; SD: Standard deviation; TXB2: Thromboxane B2; 6-keto-PGF1α: 6-keto Prostaglandin F1 alpha, VAs: Ventricular arrhythmias.

groups. The VAs group showed significantly elevated expressions of ICAM-1, VCAM-1, and caspase-3 ($p < .05$) in comparison to the normal group. Simvastatin resulted in decreased expression levels for all three markers; however, this decrease was non-significant ($p > .05$). Administration of 10 mg/kg RES further decreased ICAM-1 and VCAM-1 expression, alongside a reduction in caspase-3, but these changes were not significant ($p > .05$). The most significant impacts

($p < .05$) were observed with 50 mg/kg RES, which resulted in the lowest ICAM-1, VCAM-1, and caspase-3 expressions, indicating a protective role of RES against inflammation and apoptosis in the coronary artery (Figure 1a).

### *Kv4.2, Cav1.2, and NGF Gene Expression*

The VAs group exhibited a marked reduction ($p < .05$) in the Kv4.2, Cav1.2, and NGF expressions compared to the normal group. Treatment with simvastatin resulted in a partial recovery of Kv4.2, Cav1.2, and NGF expression levels; however, this was not significant ($p > .05$). Notably, administration of 10 mg/kg RES further improved the Kv4.2, Cav1.2, and NGF expression levels, but again, this was not significant ($p > .05$). The most significant enhancement ($p < .05$) was observed in the 50 mg/kg RES group, which demonstrated high expression levels of Cav1.2, Kv4.2, and NGF, indicating a positive effect of RES on gene expression in the left ventricle in comparison to the VAs group (Figure 1b).

### *Cav1.2, Kv4.2, and NGF Protein Expression*

Similarly, the VAs group exhibited reduced protein levels ($p < .05$) for Kv4.2, Cav1.2, and NGF compared to the normal group. Treatment with simvastatin led to a partial recovery of these protein expressions, although it was not significant ($p > .05$). Administration of 10 mg/kg RES further enhanced the protein expressions of Cav1.2, Kv4.2, and NGF, but this elevation was also non-significant ($p > .05$). The most substantial increase ($p < .05$) in Kv4.2, Cav1.2, and NGF protein expression was observed in the 50 mg/kg RES group in comparison to the VAs group, highlighting the beneficial effects of RES on protein expression in the left ventricle (Figure 2a and 2b).

## Discussion

CIHF is a complex clinical condition characterized by significant alterations in cardiac function and structure, often leading to the development of VAs. The present research indicates the therapeutic potential of RES, a polyphenolic compound, in mitigating VAs in a rat model of CIHF. RES administration not only improved lipid profiles but also reduced inflammatory markers and enhanced the expression of critical cardiac proteins and genes associated with arrhythmogenesis. The biochemical and molecular analyses conducted in this study provide insights into the multifaceted mechanisms through which RES exerts its cardioprotective effects, making it an appropriate candidate for treating arrhythmias in CIHF.

One of the critical observations in our study was the significant improvement in lipid profiles following RES treatment. Elevated levels of LDL-C and TC are well-documented risk factors for cardiovascular diseases, including CIHF. RES has been shown to exert lipid-lowering effects by inhibiting cholesterol absorption and enhancing hepatic lipid metabolism (Jia et al., 2024). Research by Faghihzadeh et al. (2014),

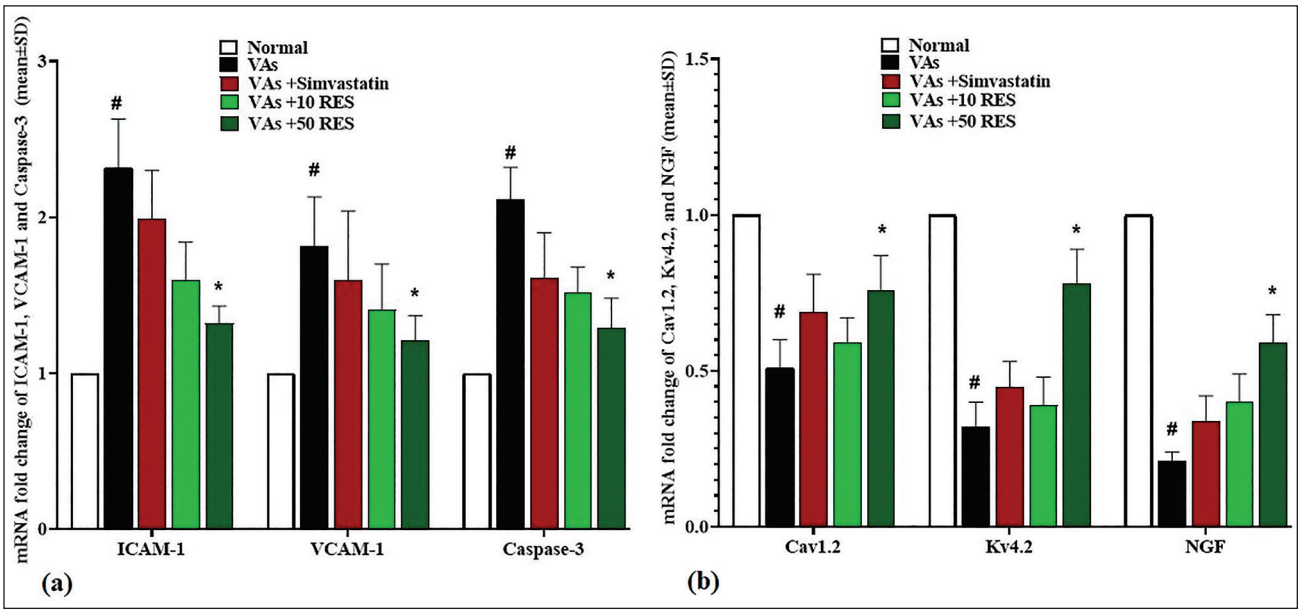



**Figure 1.** (a) Effect of RES on ICAM-1, VCAM-1, and Caspase-3 Gene Expression in the Left Anterior Descending Coronary Artery. (b) Effect of RES on Cav1.2, Kv4.2, and NGF in the Left Ventricle Gene Expression. (c) Effect of RES on Cav1.2, Kv4.2, and NGF in the Left Ventricle Protein Expression.

**Notes:** Values are mean ± SD, obtained from 10 rats. $^{\#}p < .05$, versus the normal group. $^{*}p < .05$, versus the VAs group. Cav1.2: Calcium voltage-gated channel subunit alpha1 C; ICAM-1: Intercellular adhesion molecule-1; Kv4.2: Potassium voltage-gated channel subfamily D member 2; NGF: Nerve growth factor; RES: Resveratrol; VAs: Ventricular arrhythmias; VCAM-1: Vascular cell adhesion molecule-1.

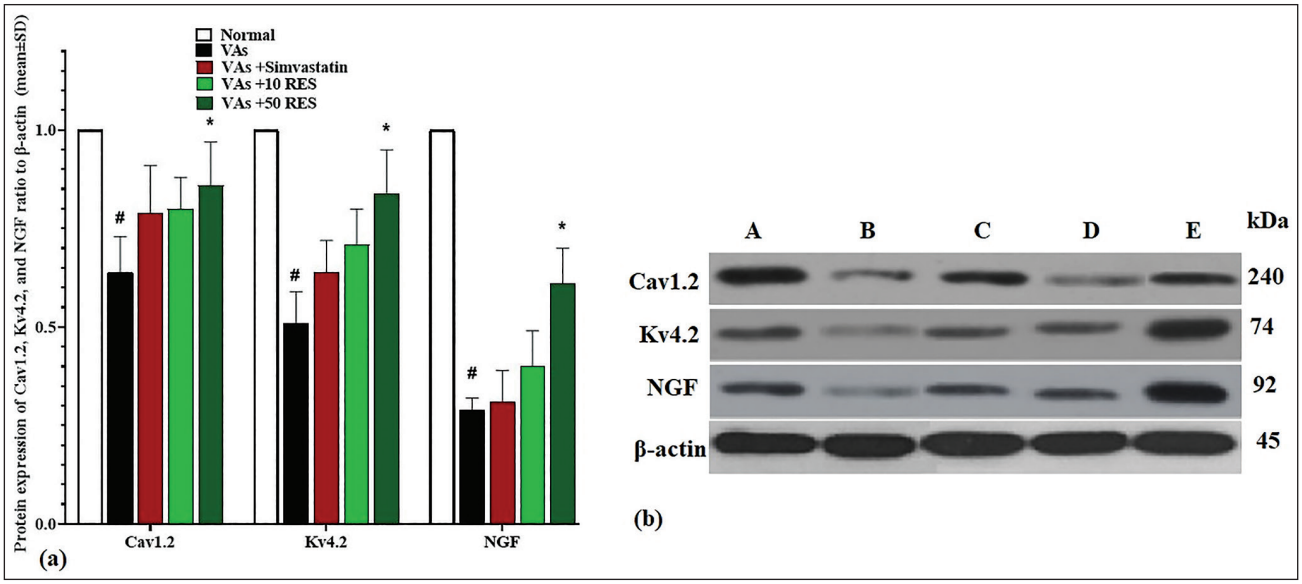



**Figure 2.** (a and b) Effect of RES on Cav1.2, Kv4.2, and NGF in the Left Ventricle Protein Expression.

**Notes:** Values are mean ± SD, obtained from 10 rats. $^{\#}p < .05$, versus the normal group. $^{*}p < .05$, versus the VAs group. Cav1.2: Calcium voltage-gated channel subunit alpha1 C; Kv4.2: Potassium voltage-gated channel subfamily D member 2; NGF: Nerve growth factor; RES: Resveratrol; VAs: Ventricular arrhythmias.

Berrougui et al. (2009), and Cao et al. (2003) found that RES regulates the lipid profiles of patients with atherosclerosis and heart failure. This regulation occurs through hormone-sensitive lipase pathways, stimulation of hepatic hepatocyte pathways, and modulation of the sympathetic nervous system, which is crucial in visceral lipogenesis, as demonstrated in randomized controlled trials. RES has shown anti-atherosclerotic effects by reducing plaque formation in arteries, improving endothelial function, and decreasing inflammation in animal models, while human studies indicate improvements in vascular health through enhanced endothelial function and reduced inflammatory markers. Our results corroborate previous findings, indicating a significant decrease in TC and LDL-C concentrations in the RES-treated groups in comparison to the VAs model group. Furthermore, the elevation in HDL-C concentrations observed with RES treatment is particularly noteworthy, as HDL-C is known for its protective role against atherosclerosis and cardiovascular events. The modulation of lipid profiles by RES may cause the stabilization of cardiac function and reduction of arrhythmogenic potential, emphasizing the importance of managing dyslipidemia in CIHF patients (Darwish et al., 2021).

Besides its effects on lipid metabolism, RES demonstrated potent anti-inflammatory properties, significantly reducing levels of inflammatory cytokines, like IL-8, IL-1β, and TNF-α (Li et al., 2021). Chronic inflammation is a hallmark of CIHF, contributing to myocardial damage and remodeling, which predisposes patients to VAs. Atherosclerosis, CIHF, and arrhythmias are chronic inflammatory diseases identified by many important molecules, including IL-1β, TNF-α, CRP, and IL-8 (Stone et al., 2023). Elevated levels of these markers were found in VAs rats (Shi et al., 2023). Notably, IL-1β and TNF-α levels were markedly reduced in the VAs + RES group versus the VAs group, and IL-8 levels also dropped significantly with RES treatment. Thus, RES's anti-atherosclerotic effects are linked to its ability to suppress inflammatory responses in these rats. Endothelial dysfunction, an early indicator of atherosclerosis, is associated with 6-keto-PGF1α, NO, ET, and TXB2 levels (Ziyu et al., 2023). Compared to the normal group, decreased 6-keto-PGF1α and NO concentrations alongside increased TXB2 and ET concentrations were detected in the VAs group. After RES treatment, TXB2 and ET concentrations decreased while 6-keto-PGF1α concentrations increased, suggesting that RES administration benefits VAs rats by protecting endothelial function. The upregulation of adhesion molecules, such as VCAM-1 and ICAM-1, observed in the VAs model, facilitates leukocyte infiltration into the myocardium, exacerbating inflammation and fibrosis. RES treatment effectively downregulated the expression of these adhesion molecules, suggesting a protective role against myocardial inflammation. The reduction in inflammatory markers aligns with the observed decrease in caspase-3 expression, indicating a potential anti-apoptotic effect of RES. By mitigating inflammation and apoptosis, RES may enhance myocardial resilience and stability, thereby reducing the incidence of VAs in the context of CIHF.

Atherosclerosis is a chronic inflammatory disease characterized by several key molecules, including CRP (a cardiovascular disease marker), TNF-α, IL-1β (an important factor in the AS inflammatory pathway), and IL-8 (crucial for monocyte recruitment). Elevated levels of these markers were found in AS rats (Sinitsky et al., 2020; Tyrrell &

Goldstein, 2021). Notably, TNF-α and IL-1β levels significantly decreased in the AS + RAL group compared to the AS group, and IL-8 levels also dropped significantly with RAL treatment. Thus, RAL's anti-atherosclerotic effects are linked to its ability to suppress inflammatory responses in these rats. Endothelial dysfunction, an early indicator of atherosclerosis, is associated with levels of NO, 6-keto-PGF1α, ET, and TXB2 (Yu et al., 2022). Compared to the normal group, the AS group showed decreased NO and 6-keto-PGF1α levels alongside increased ET and TXB2 levels. After RAL treatment, ET and TXB2 levels decreased while 6-keto-PGF1α levels increased, suggesting that RAL administration benefits AS rats by protecting endothelial function. The RAL is known for its high polyphenol content, with various compounds exhibiting biological effects on cardiovascular health. For instance, hyperoside and rutin enhance coronary flow, while rutin, chlorogenic acid, isoquercitrin, and epicatechin reduce TBARS in $Cu^{2+}$-induced LDL oxidation. Procyanidin B2 can inhibit the proliferation and migration of human aortic smooth muscle cells induced by advanced glycation end products (Khaliq et al., 2023; Li et al., 2022). These compounds are believed to contribute significantly to the anti-atherosclerotic properties of RAL.

## Conclusion

Our study demonstrates that RES exerts significant anti-arrhythmic effects in a rat model of CIHF through multiple mechanisms, including lipid modulation, anti-inflammatory activity, and endothelial protection. The treatment with RES notably improved lipid profiles by reducing TC and low-density lipoprotein levels while increasing high-density lipoprotein levels. Furthermore, RES effectively diminished inflammatory cytokines and adhesion molecules, which are critical in the pathogenesis of VAs. The upregulation of Cav1.2, Kv4.2, and NGF expression in the left ventricle suggests that RES enhances cardiac electrical stability, potentially mitigating the risk of VAs. While these findings highlight the promising role of RES as a therapeutic agent for managing arrhythmias in CIHF, the study acknowledges limitations, such as the need for further research to validate these results in human subjects and explore the long-term effects of RES treatment. Overall, this investigation underscores the novel impact of RES on cardiac health and its potential clinical applications in preventing arrhythmias associated with chronic heart failure.

### Abbreviations

CAT: Catalase; CIHF: Chronic ischemic heart failure; ET: Endothelin; GSH-Px: Glutathione peroxidase; HDL-C: High-density lipoprotein cholesterol; ICAM-1: Intercellular adhesion molecule-1; IL-1β: Interleukin-1 beta; IL-8: Interleukin-8; LDL-C: Low-density lipoprotein cholesterol; MI: Myocardial infarction; MDA: Malondialdehyde; NGF: Nerve growth factor; NO: Nitric oxide; PCR: Polymerase chain reaction; RES: Resveratrol; RIA: Radioimmunoassay; SCD: Sudden cardiac death; SOD: Superoxide dismutase; TBARS: Thiobarbituric acid-reactive substances; TC: Total cholesterol; TG: Triglycerides; TXB2: Thromboxane B2; VAs: Ventricular arrhythmias; VCAM-1: Vascular cell adhesion molecule-1.

### Declaration of Conflicting Interests

The authors declared no potential conflicts of interest with respect to the research, authorship, and/or publication of this article.

### Ethical Approval

The experimental protocols of this study were approved by Xi'an Gaoling Hospital.

### Funding

The authors disclosed receipt of the following financial support for the research, authorship, and/or publication of this article: This study was supported by Jilin Province Health and Wellness Science and Technology Capacity Enhancement Program Project (2025WSKA021) with project name: Correlation Study between SPECT Bone Imaging and Oxidative Stress Indicators in Patients with Bone Metastasis of Lung Cancer.

### Informed Consent

Not applicable.

### ORCID iD

Yan Wang https://orcid.org/0009-0000-6619-5216

### References

Aguilar, I. K., Arias-Ruiz, H., Alnsour, S., Frishman, W. H., & Aronow, W. S. (2025). Electrophysiologic ablation of ventricular tachyarrhythmias. *Cardiology in Review*. https://doi.org/10.1097/CRD.0000000000001015

Bei, Y.-R., Zhang, S.-C., Song, Y., Tang, M.-L., Zhang, K.-L., Jiang, M., He, R.-C., Wu, S.-G., Liu, X.-H., Wu, L.-M., Dai, X.-Y., & Hu, Y.-W. (2023). EPSTI1 promotes monocyte adhesion to endothelial cells *in vitro via* upregulating VCAM-1 and ICAM-1 expression. *Acta Pharmacologica Sinica*, *44*(1), 71–80. https://doi.org/10.1038/s41401-022-00923-5

Berrougui, H., Grenier, G., Loued, S., Drouin, G., & Khalil, A. (2009). A new insight into resveratrol as an atheroprotective compound: Inhibition of lipid peroxidation and enhancement of cholesterol efflux. *Atherosclerosis*, *207*(2), 420–427.

Cao, H., Pan, X., Li, C., Zhou, C., Deng, F., & Li, T. (2003). Density functional theory calculations for resveratrol. *Bioorganic & Medicinal Chemistry Letters*, *13*(11), 1869–1871.

Chen, H., Zhang, S., Wang, H., Bao, L., Wu, W., & Qi, R. (2022). Fruitflow inhibits platelet function by suppressing Akt/GSK3β, Syk/PLCγ2 and p38 MAPK phosphorylation in collagen-stimulated platelets. *BMC Complementary Medicine and Therapies*, *22*(1), 75.

Crowell, J. A., Korytko, P. J., Morrissey, R. L., Booth, T. D., & Levine, B. S. (2004). Resveratrol-associated renal toxicity. *Toxicological Sciences*, *82*(2), 614–619.

Czyż, Ł., Chmiel, J., Drabik, L., Mazurek, A., Kwiecień, E., Sikorska, M., Skubera, M., Kozynacka, A., Olszowska, M., Zasada, W., Podolec, P., & Musiałek, P. (2022). Eligible-and-enrolled vs. eligible-but-not-enrolled patients with chronic ischaemic heart failure in randomized clinical trials of myocardial regeneration. *Advances in Interventional Cardiology/Postępy w Kardiologii Interwencyjnej*, *18*(4), 407–415.

Darwish, M. A., Abdel-Bakky, M. S., Messiha, B. A., Abo-Saif, A. A., & Abo-Youssef, A. M. (2021). Resveratrol mitigates pancreatic TF activation and autophagy-mediated beta cell death via inhibition of CXCL16/ox-LDL pathway: A novel protective mechanism against type 1 diabetes mellitus in mice. *European Journal of Pharmacology*, *901*, 174059.

Dokshokova, L., Franzoso, M., Di Bona, A., Moro, N., Sanchez Alonso, J. L., Prando, V., Sandre, M., Basso, C., Faggian, G., Abriel, G., Marin, O., Gorelik, J., Zaglia, T., & Mongillo, M. (2022). Nerve growth factor transfer from cardiomyocytes to innervating sympathetic neurons activates TrkA receptors at the neuro-cardiac junction. *The Journal of Physiology*, *600*(12), 2853–2875.

Faghihzadeh, F., Adibi, P., Rafiei, R., & Hekmatdoost, A. (2014). Resveratrol supplementation improves inflammatory biomarkers in patients with nonalcoholic fatty liver disease. *Nutrition Research*, *34*(10), 837–843.

Fan, S., Hu, Y., You, Y., Xue, W., Chai, R., Zhang, X., Shou, X., & Shi, J. (2022). Role of resveratrol in inhibiting pathological cardiac remodeling. *Frontiers in Pharmacology*, *13*, 924473.

Guo, Y., Zhang, C., Ye, T., Chen, X., Liu, X., Chen, X., Sun, Y., Qu, C., Liang, J., Shi, S., & Yang, B. (2021). Pinocembrin ameliorates arrhythmias in rats with chronic ischaemic heart failure. *Annals of Medicine*, *53*(1), 830–840.

Hosoda, R., Nakashima, R., Yano, M., Iwahara, N., Asakura, S., Nojima, I., Asakura, S., Nojima, I., Saga, Y., Kunimoto, R., Horio, Y., & Kuno, A. (2023). Resveratrol, a SIRT1 activator, attenuates aging-associated alterations in skeletal muscle and heart in mice. *Journal of Pharmacological Sciences*, *152*(2), 112–122.

Jia, Y. P., Wang, J. M., Lyu, J. Q., Yang, H. H., Miao, M. Y., Wang, X., Wan, Z.-X., Zheng, Y., Qin, L.-Q., Li, F.-R., & Chen, G. C. (2024). Triglyceride-rich lipoproteins cholesterol, 10-years atherosclerotic cardiovascular disease risk, and risk of myocardial infarction and ischemic stroke. *Journal of Lipid Research*, *65*(11), 100653.

Kapetanovic, I. M., Muzzio, M., Huang, Z., Thompson, T. N., & McCormick, D. L. (2011). Pharmacokinetics, oral bioavailability, and metabolic profile of resveratrol and its dimethylether analog, pterostilbene, in rats. *Cancer Chemotherapy and Pharmacology*, *68*(3), 593–601.

Khaliq, T., Akhter, S., Sultan, P., & Hassan, Q. P. (2023). Critical review on *Rumex dentatus* L. a strong pharmacophore and the future medicine: Pharmacology, phytochemical analysis and traditional uses. *Heliyon*, *9*(3), Article e14159. https://doi.org/10.1016/j.heliyon.2023.e14159

Lan, S., Yang, B., Migneault, F., Turgeon, J., Bourgault, M., Dieudé, M., Cardinal, H., Hickey, M. J., Patey, N., & Hébert, M. J. (2021). Caspase-3-dependent peritubular capillary dysfunction is pivotal for the transition from acute to chronic kidney disease after acute ischemia-reperfusion injury. *American Journal of Physiology-Renal Physiology*, *321*(3), F335–F351.

Lankin, V. Z., Tikhaze, A. K., & Melkumyants, A. M. (2022). Malondialdehyde as an important key factor of molecular mechanisms of vascular wall damage under heart diseases development. *International Journal of Molecular Sciences*, *24*(1), 128.

Li, B. W., Liu, Y., Zhang, L., Guo, X. Q., Wen, C., Zhang, F., Luo, X.-Y., & Xia, Y. P. (2021). Cytotoxin-associated gene A (CagA) promotes aortic endothelial inflammation and accelerates atherosclerosis through the NLRP3/caspase-1/IL-1β axis. *The FASEB Journal*, *35*(11), e21942.

Li, J.-J., Li, Y.-X., Li, N., Zhu, H.-T., Wang, D., & Zhang, Y.-J. (2022). The genus *Rumex* (Polygonaceae): An ethnobotanical, phytochemical and pharmacological review. *Natural Products and Bioprospecting*, *12*(1), 21. https://doi.org/10.1007/s13659-022-00346-z

Liu, Z., Song, Y., Zhang, X., Liu, Z., Zhang, W., Mao, W., & Liu, C. (2005). Effects of trans-resveratrol on hypertension-induced cardiac hypertrophy in a partially nephrectomized rat model. *Clinical and Experimental Pharmacology and Physiology*, *32*(12), 1049–1054.

Liu, Z., Xin, H., & Chopp, M. (2021). Axonal remodeling of the corticospinal tract during neurological recovery after stroke. *Neural Regeneration Research*, *16*(5), 939–943.

Liu, T., Hao, Y., Zhang, Z., Zhou, H., Peng, S., Zhang, D., Li, K., Chen, Y., & Chen, M. (2024). Advanced cardiac patches for the treatment of myocardial infarction. *Circulation*, *149*(25), 2002–2020.

Mavrogeni, S., Piaditis, G., Bacopoulou, F., & Chrousos, G. P. (2022). Cardiac remodeling in hypertension: Clinical impact on brain, heart, and kidney function. *Hormone and Metabolic Research*, *54*(5), 273–279.

Muñoz-Prieto, A., Pardo-Marín, L., Goyena, E., García Manzanilla, E., Cerón, J. J., & Franco-Martínez, L. (2025). Changes of cytokines in saliva of pigs with streptococcus suis infection measured with a multiplex assay. *Veterinary Sciences*, *12*(4), 316.

Naseri, L., Khazaei, M., Ghanbari, E., & Bazm, M. A. (2019). *Rumex alveollatus* hydroalcoholic extract protects CCL4-induced hepatotoxicity in mice. *Comparative Clinical Pathology*, *28*(2), 557–565. https://doi.org/10.1007/s00580-018-2846-7

Qian, J., Song, T., Zhang, Q., Cai, G., & Cai, M. (2024). Analysis and diagnosis of hemolytic specimens by AU5800 biochemical analyzer combined with AI technology. *Frontiers in Computing and Intelligent Systems*, *6*(3), 100–103.

Raj, P., Thandapilly, S. J., Wigle, J., Zieroth, S., & Netticadan, T. (2021). A comprehensive analysis of the efficacy of resveratrol in atherosclerotic cardiovascular disease, myocardial infarction and heart failure. *Molecules*, *26*(21), 6600.

Salari, N., Morddarvanjoghi, F., Abdolmaleki, A., Rasoulpoor, S., Khaleghi, A. A., Hezarkhani, L. A., Shohaimi, S., & Mohammadi, M. (2023). The global prevalence of myocardial infarction: A systematic review and meta-analysis. *BMC Cardiovascular Disorders*, *23*(1), 206.

Shi, H., Zhao, Y., Li, S., Wu, H., Ma, D., & Wan, C. (2023). TNF-α and IL-8 levels are positively correlated with hypobaric hypoxic pulmonary hypertension and pulmonary vascular remodeling in rats. *Open Life Sciences*, *18*(1), 20220650.

Singh, V., Kaur, R., Kumari, P., Pasricha, C., & Singh, R. (2023). ICAM-1 and VCAM-1: Gatekeepers in various inflammatory and cardiovascular disorders. *Clinica Chimica Acta; International Journal of Clinical Chemistry*, *548*, Article 117487. https://doi.org/10.1016/j.cca.2023.117487

Sinitsky, M. Y., Tsepokina, A. V., Kutikhin, A. G., Shishkova, D. K., & Ponasenko, A. V. (2020). Secretion and gene expression

of proatherosclerotic cytokines IL6 and IL8 by endothelial cells exposed to mutagen. *Journal of Medical Genetics*, *19*(12), 38–46.

Song, S., Tien, C. L., Cui, H., Basil, P., Zhu, N., Gong, Y., Li, W., Li, H., Fan, Q., Choi, J. M., Luo, W., Xue, Y., Cao, R., Zhou, W., Ortiz, A. R., Stork, B., Mundra, V., Putluri, N., York, B., & Sun, Z. (2022). Myocardial REV-ERB-mediated diurnal metabolic rhythm and obesity paradox. *Circulation*, *145*(6), 448–464.

Stone, P. H., Libby, P., & Boden, W. E. (2023). Fundamental pathobiology of coronary atherosclerosis and clinical implications for chronic ischemic heart disease management—The plaque hypothesis: A narrative review. *JAMA Cardiology*, *8*(2), 192–201.

Theodorakis, N., Feretzakis, G., Kreouzi, M., Anagnostou, D., Hitas, C., Verykios, V. S., & Nikolaou, M. (2025). GH therapy in chronic heart failure: A systematic review and meta-analysis of randomized controlled trials. *The Journal of Clinical Endocrinology & Metabolism*, *110*(4), e1252–e1260.

Tyrrell, D. J., & Goldstein, D. R. (2021). Ageing and atherosclerosis: Vascular intrinsic and extrinsic factors and potential role of IL-6. *Nature Reviews. Cardiology*, *18*(1), 58–68. https://doi.org/10.1038/s41569-020-0431-7

Wittenbecher, C., Eichelmann, F., Toledo, E., Guasch-Ferre, M., Ruiz-Canela, M., Li, J., Arós, F., Lee, C.-H., Liang, L., Salas-Salvadó, J., Clish, C. B., Schulze, M. B., Martínez-González, A. M., & Hu, F. B. (2021). Lipid profiles and heart failure risk: results from two prospective studies. *Circulation Research*, *128*(3), 309–320.

Wu, L. Y., Song, Y. J., Zhang, C. L., & Liu, J. (2023). KV channel-interacting proteins in the neurological and cardiovascular systems: An updated review. *Cells*, *12*(14), 1894.

Xiang, Y. T., Xing, X. X., Hua, X. Y., Zhang, Y. W., Xue, X., Wu, J. J., Zheng, M.-X., Wang, H., & Xu, J. G. (2023). Altered neural pathways and related brain remodeling: A rat study using different nerve reconstructions. *Neurosurgery*, *93*(1), 233–243.

Yu, L., Liu, H., Ma, X., Seshadri, V. D., & Gao, X. (2022). Anti-atherosclerotic effects of myrtenal in high-fat diet-induced atherosclerosis in rats. *Applied Biochemistry and Biotechnology*, *194*(12), 5717–5733. https://doi.org/10.1007/s12010-022-04044-x

Zhao, X., Wang, D., & Qin, L. (2021). Lipid profile and prognosis in patients with coronary heart disease: A meta-analysis of prospective cohort studies. *BMC Cardiovascular Disorders*, *21*, 1–15.

Ziyu, C. H. E. N., Nuoyan, W. E. I., Zhishan, L. I. A. N. G., Xiuwen, H. U., Junyi, W. A. N. G., Qingsong, C. H. E. N., & Hongyu, Y. A. N. G. (2023). Expression changes of prostacyclin and thromboxane in blood of rats with tail vibration. *Journal of Environmental and Occupational Medicine*, *39*(11), 1226–1230.